

- Eksp. Teor. Fiz. 62, 614 (1972); 64, 813 (1973) [Sov. Phys. JETP 35, 325 (1972); 37, 413 (1973)].
- ¹⁰Physical Acoustics (ed. by W. Mason and R. Thurston), Vol. 6, Academic Press, New York, 1970 (Russ. Transl., Mir, 1973).
- ¹¹V. A. Alekseev, B. Ya. Zel'dovich, and I. I. Sobel'man, *Kvantovaya Elektron. (Moscow)* 2, 1007 (1975) [Sov. J. Quantum Electron. 5, 547 (1975)].
- ¹²P. Jacquinot, *J. Opt. Soc. Am.* 44, 761 (1954).
- ¹³W. G. Schweitzer, Jr., E. G. Kessler, Jr., R. D. Deslattes, H. P. Layer, and J. R. Whetstone, *Appl. Opt.* 12, 2927 (1973).
- ¹⁴M. S. Sorem and A. L. Schawlow, *Opt. Commun.* 5, 148 (1972).
- ¹⁵G. R. Hanes, J. Lapierre, P. R. Bunker, and K. C. Shotton, *J. Mol. Spectrosc.* 39, 506 (1971).
- ¹⁶S. É. Frish, *Opticheskie spektry atomov (Optical Spectra of Atoms)*, Nauka, 1963.

Translated by A. K. Ageyi

Selective two-step ionization of rubidium by laser radiation

R. V. Ambartsumyan, A. M. Apatin, V. S. Letokhov, A. A. Makarov,
V. I. Mishin, A. A. Puretskii, and N. P. Furzikov

Institute of Spectroscopy, USSR Academy of Sciences
(Submitted September 13, 1975)
Zh. Eksp. Teor. Fiz. 70, 1660-1673 (May 1976)

Selective application of pulsed laser radiation from dye and ruby lasers was used to produce two-step ionization of rubidium atoms with initial ion density of about 10^{13} cm^{-3} per pulse. Every excited atom of rubidium was ionized, i.e., radiation-intensity saturation was achieved for the second step. The yield of ions as a function of the exciting and ionizing intensities and of the density of atoms was investigated both experimentally and theoretically. This analysis was used as a basis for a simple method of measuring the photoionization cross sections for atoms in excited states, which did not require a knowledge of the absolute number of excited atoms. The method was used to measure the cross sections for photoionization from the 6^2P state of the Rb atom by fundamental-frequency radiation from a ruby laser [$\sigma_2 = (1.7 \pm 0.3) \times 10^{-17} \text{ cm}^2$] and the second-harmonic radiation from a ruby laser [$\sigma_2 = (0.19 \pm 0.03) \times 10^{-17} \text{ cm}^2$].

PACS numbers: 32.10.Qy

1. INTRODUCTION

The exceedingly small spectral width of a laser line makes the laser a very precise instrument for the selective interaction with matter, and the high intensity of laser radiation ensures that this interaction occurs very efficiently. Two-step ionization is one of the most universal methods of selective interaction between laser radiation and atoms and molecules. It was first proposed and used in^[1,2]. Its principle is as follows. Laser radiation at frequency ν_1 is absorbed by atoms of a selected type (for example, atoms of the required isotopic composition or those containing nuclei of a particular isomer, or simply atoms of a particular element), and transitions to the excited state take place. A second laser operating at frequency ν_2 is then used to ionize the selectively excited atoms, and this second frequency is chosen so that atoms still in the ground state are not ionized.

Selective two-step ionization of atoms by laser radiation is now regarded as a universal method for isotope separation, for producing ultrapure materials, and for the separation of atoms containing isomeric nuclei.^[3] The method has been used to separate the isotopes of uranium,^[4] calcium,^[5] and magnesium.^[6] However, the last three papers were concerned only with the possibility of separating isotopes by two-step ionization by laser radiation, and the ion densities produced by this selective process did not exceed 10^6 cm^{-3} .

In a practical application of the process, on the other hand, one must produce high densities of selectively generated ions ($10^{12} - 10^{14} \text{ cm}^{-3}$). Resonance charge exchange with typical cross sections in the range $10^{-14} - 10^{-15} \text{ cm}^2$ ^[7] imposes an essential restriction on the upper limit of possible densities. Moreover, the process must be carried out so that each atom of the selected type is ionized, and each selectively produced ion is removed from plasma. We have succeeded, for the first time, in using the selective interaction between laser radiation and rubidium atoms to produce plasma with a density of 10^{13} cm^{-3} . The extraction of ions produced in this way by an electric field has been investigated. Every excited atom in the volume under investigation was ionized, i.e., intensity saturation was achieved for the second step.

Before the method of selective two-step ionization of atoms by laser radiation can be used, one must know the cross sections for the photoexcitation and photoionization of atoms from excited states. The photoionization cross sections are well known,^[8] but the cross sections for photoionization from excited states are practically unknown.^[9] Whenever such measurements have been performed,^[10,11] they required a knowledge of the absolute number of excited atoms, and this was difficult to determine. In this paper, we propose a simple method of measuring the cross sections for photoionization from excited states, which is based

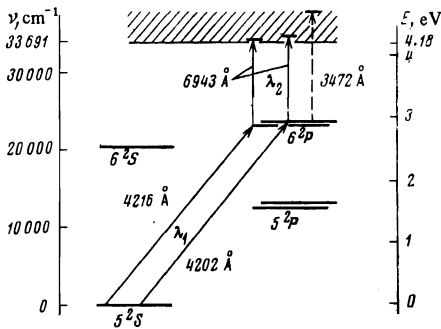


FIG. 1. Energy level scheme for the rubidium atom and the working transitions.

on the saturation of the ion photocurrent as a function of the intensity corresponding to the second step, and which does not require a knowledge of the absolute number of excited atoms. The photoionization cross sections have been measured for rubidium atoms in the $6^2P_{3/2}$, and $6^2P_{1/2}$ states for ~ 1.8 and 3.6 eV incident-photon energies.

2. EXPERIMENTAL ARRANGEMENT AND METHOD

We have investigated experimentally the two-step ionization of rubidium atoms by selective excitation of the components of the 6^2P doublet, using a tunable dye laser ($\nu_1 = 23\,799$ or $23\,725$ cm^{-1}) and the simultaneous ionization of the excited atoms by ruby laser radiation ($\nu_2 = 14\,403$ cm^{-1}) or the second harmonic radiation ($\nu_2 = 28\,806$ cm^{-1}). The energy-level scheme for the rubidium atom and the working transitions are shown in Fig. 1.

The experimental setup is illustrated in Fig. 2. It consisted of the following main parts: ruby laser (1), dye laser (2), rubidium vapor cell (3), and ion-current measuring system (4). The Q-switched ruby laser generated a 20-nsec pulse carrying an energy of 0.5 J at a repetition frequency of 5 Hz. The energy carried by the second-harmonic pulse from the ruby laser was 0.015 J. Some of this radiation was used to pump the dye laser. The narrow-band tunable dye laser (solution of POPOP in toluene) was based on the standard schemes.^[12] The laser cavity was formed by a 1200-line/mm diffraction grating working in the first order and a flat mirror with a reflection coefficient of 30%. The cavity length was 0.5 m. A telescope with a magnification of $25\times$ was placed in the cavity to ensure that the aperture of the grating was filled and the divergence of the radiation incident upon it was reduced. The windows of the cell containing the dye solution were inclined at 6° to the optical axis. The dye solution was flushed through the cell at a rate of 0.5 liter/sec. Wavelength variation was achieved by rotating the grating.

The second-harmonic radiation from the ruby laser was used to pump the dye laser. The transverse pumping scheme was employed in which the second-harmonic radiation was focused on the cell containing the dye solution by a cylindrical quartz lens with a focal length of 9 cm. Under these conditions, the dye laser produced 1 kW for a pulse length of about 20 nsec. The

width of the spectrum was measured with a Fabry-Perot interferometer having a dispersion band of 2.5 cm^{-1} , and was found to be about 0.5 cm^{-1} .

The rubidium vapor was held in a glass cell with plane-parallel windows. 99.9% pure metallic rubidium was introduced into a vacuum of 10^{-5} Torr through a side tube in the cell. The cell was located in a heater designed so that the temperature of the side tube was lower than the temperature of the cell by 20°C . The vapor pressure P was then determined by the temperature of this tube. The cell windows were maintained at a higher temperature than the rest of the cell in order to prevent condensation of rubidium vapor. The cell was continuously pumped, and the pressure inside it was held at 10^{-4} Torr. Brass electrodes, 2 cm in diameter and 1 cm apart, were fixed inside the cell on molybdenum leads.

The ion current was measured by a collecting capacitor ($C_0 = 0.25$ pF), with one of its electrodes held at a constant potential U , a load resistor ($R_l = 100$ k Ω), and an S8-2 oscillograph. The signal recorded by the oscillograph can be described by the following formula:

$$u = \frac{\Delta q}{C_0 + C_p} \exp\left(-\frac{t}{R_l(C_0 + C_p)}\right), \quad (2.1)$$

where u is the potential difference across the load resistance R_l , Δq is the charge produced in the space between the capacitor electrodes, C_p is the parasitic capacitance, and t is the time. The parasitic capacitance was found to be 420 pF. The total recorded number of ions was calculated from the amplitude of the voltage pulse given by (2.1), using the formula $N_i = 2.9 \times 10^9 u$, where u is the pulse amplitude in volts.

The exciting and ionizing radiations were introduced into the cell in opposite directions and were limited by stops, 2.6 mm in diameter (see Fig. 2).

The background signal during ionization by the fundamental-frequency radiation from the ruby laser did not exceed 10 mV (2.9×10^7 ions). In the case of ionization by the second-harmonic radiation, the background signal was found to increase linearly with increasing rubidium vapor density in the cell and the intensity of the second harmonic. It was found to be 30–50% of the

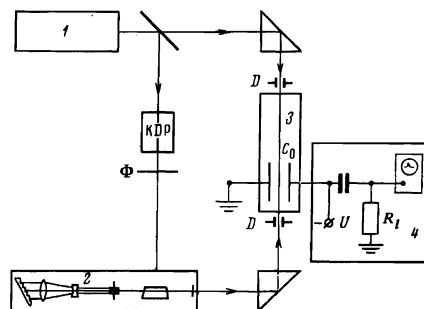


FIG. 2. Experimental setup: 1—ruby laser; 2—dye laser; 3—cell containing rubidium vapor; 4—ion detection system. (C_0 —recording capacitance, R_l —load resistance, U —voltage between electrodes, F—filter, KDP nonlinear crystal, D—beam stop).

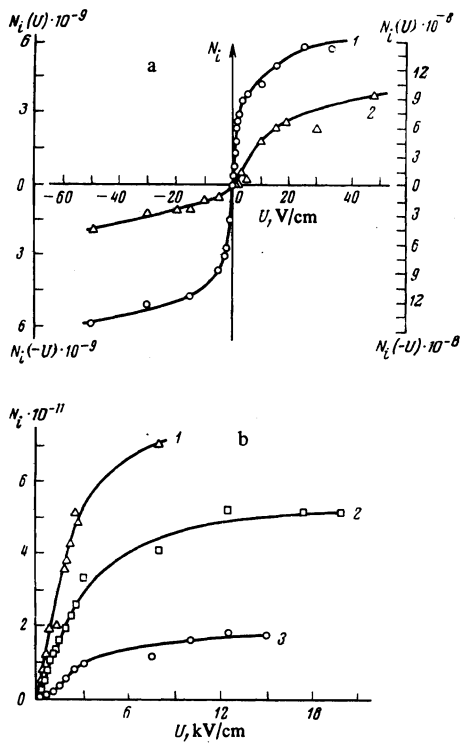


FIG. 3. Total number of recorded ions N_i as a function of field strength. a) Small values of U : curve 1 (left-hand scale)—ionization by ruby laser radiation ($\nu_2 = 14\,403\text{ cm}^{-1}$), curve 2 (right-hand scale)—ionization by second-harmonic radiation from the ruby laser ($\nu_2 = 28\,806\text{ cm}^{-1}$). Frequency of exciting radiation $\nu_1 = 23\,799\text{ cm}^{-1}$, rubidium-atom density in the cell $N_0 = 2.9 \times 10^{13}\text{ cm}^{-3}$. b) Large values of U : curve 1—rubidium atom density in the cell $N_0 = 2 \times 10^{14}\text{ cm}^{-3}$, curve 2— $N_0 = 7.6 \times 10^{13}\text{ cm}^{-3}$, curve 3— $N_0 = 2.9 \times 10^{13}\text{ cm}^{-3}$.

resultant signal. The resonance signal in this case was determined as the difference between the resultant and background signals. The amplitude of the background signal was determined by detuning the exciting dye-laser radiation from the absorption line of the rubidium vapor. The width of the resonance in the ion current was about 0.5 cm^{-1} (full width at half height) and was equal to the dye-laser linewidth.

3. EXTRACTION OF IONS BY AN ELECTRIC FIELD

The simultaneous exposure of the rubidium vapor to the frequencies ν_1 ($23\,799\text{ cm}^{-1}$) and ν_2 ($14\,403\text{ cm}^{-1}$) led to selective ionization of the rubidium atoms, and the energy of the laser radiation was sufficient to produce a plasma in the space between the electrodes.

Figure 3a shows the total number of recorded ions as a function of the potential difference between the electrodes (separated by 1 cm). Curves 1 and 2 correspond to cases where the energy of the ionizing photon was 0.56 and 2.3 eV above the ionization limit, respectively. Figure 3b shows the total number of recorded ions as a function of the potential difference between the electrodes for large negative values of the potential on one of the electrodes. Curves 1–3 were obtained for different rubidium-vapor densities in the cell. It is clear

that these characteristics reach saturation and, moreover, as the rubidium vapor density increases, a higher electric field is necessary for the complete extraction of the ions. The necessary electric field is about 10^4 V/cm for a maximum total number of ions $N_i \sim 10^{12}$ per pulse (the ion density at the initial instant of time was $n_i \sim 10^{13}\text{ cm}^{-3}$, curve 1 in Fig. 3b).

We have also investigated the total number of recorded ions as a function of the electric field for different intensities of the laser radiation corresponding to the first step. We found that, when the first-step radiation intensity was attenuated by a factor of 100, this dependence became saturated for electric fields of about $1.8 \times 10^3\text{ V/cm}$ between the electrodes. The rubidium-atom density in the cell was then $4.4 \times 10^{12}\text{ cm}^{-3}$, and the recorded number of ions at saturation was about 2×10^{10} .

Analysis of the current-voltage characteristics (Fig. 3a) by the double-probe method^[13] showed that the electron temperature of the plasma for curves 1 and 2 was 0.48 and 1.4 eV, respectively.

In the case of photoionization of rubidium atoms by laser radiation, the energy excess ΔE above the ionization limit is carried off by the liberated electrons ($M_i \gg m_e$), so that ions and monoenergetic electrons with kinetic energy ΔE are formed at the initial instant of time. However, even for plasma densities of $\sim 10^{12}\text{ cm}^{-3}$, the Maxwellization of the electron component occurs in a time $\tau_M \sim 7\text{ nsec}$ and, under these conditions, $\tau_M \sim n_e^{-1}$ ^[14] (n_e is the electron density).

Thus, before the laser pulse is over ($\tau_p \sim 20\text{ nsec}$), the electron component succeeds in reaching the Maxwell distribution, and the electron temperature $T_e = \frac{2}{3}\Delta E$ is established. For ΔE corresponding to the ionization frequencies ν_1 and ν_2 , this yields electron temperatures of the order of 0.37 and 1.53 eV, which is in good agreement with values obtained experimentally (Fig. 3a, curves 1 and 2).

Further interpretation of the experimental results will require formulas giving the ion yield as a function of the radiation intensity and the density of atoms.

4. KINETICS OF TWO-STEP PHOTOIONIZATION

We shall now consider the kinetics of the two-step photoionization of atoms, subject to the following assumptions which correspond to the experimental conditions: (a) in addition to the two-step transitions induced by the laser radiations, there is also spontaneous decay to the ground state at the rate A and spontaneous decay to the intermediate states at the rate A^* ; (b) all types of relaxation by collision can be neglected; (c) absorption of laser radiation corresponding to the first step in the direction of propagation is taken into account, and (d) the medium is assumed to be optically thin for the laser radiation corresponding to the second step. Under these assumptions, the set of equations for the populations n_1 (ground state) and n_2 (excited state) and for the intensity I_1 of radiation corresponding to the first step has the form

$$\begin{aligned} \frac{\partial n_1}{\partial t} &= -\sigma_1 I_1 \left(n_1 - \frac{n_2}{g} \right) + A n_2, \\ \frac{\partial n_2}{\partial t} &= \sigma_1 I_1 \left(n_1 - \frac{n_2}{g} \right) - A n_2 - A' n_2 - \sigma_2 I_2 n_2, \\ \frac{\partial I_1}{\partial z} + \frac{1}{c} \frac{\partial I_1}{\partial t} &= -\sigma_1 I_1 \left(n_1 - \frac{n_2}{g} \right). \end{aligned} \quad (4.1)$$

In these expressions, σ_1 is the total absorption cross section for the working transition, σ_2 is the cross section for the photoionization of the atom from the excited state, $g = g_2/g_1$ is the ratio of the statistical weights of the excited and ground states, and the intensities I_1 and I_2 are expressed in photons/cm² · sec.

Let us suppose that the laser radiation pulse is rectangular in shape and that its leading edge passes through the boundary of the medium ($z = 0$) at time $t = 0$. We shall use the new variable $\tau = t - z/c$ and the following substitutions:

$$\sigma_1 I_1 = W_1, \quad \sigma_1 I_1|_{z=0} = V_1, \quad \sigma_2 I_2 = V_2, \quad B = A + V_2. \quad (4.2)$$

In terms of the new notation, and subject to the initial and boundary conditions

$$n_1|_{\tau=0} = n_0, \quad n_2|_{\tau=0} = 0, \quad W_1|_{z=0} = V_1 = \text{const}$$

($0 < \tau < \tau_p$), the set of equations given by (4.1) can be reduced by the standard method^[15] (see Appendix) to the following differential equation for the function $W_1(\tau)$:

$$\frac{d}{d\tau} \left(\frac{1}{W_1} \frac{dW_1}{d\tau} \right) + \frac{g+1}{g} \frac{dW_1}{d\tau} + \frac{A+B}{W_1} \frac{dW_1}{d\tau} + BW_1 = BV_1. \quad (4.3)$$

The variable z is present in the initial conditions for (4.3) as a parameter:

$$W_1|_{\tau=0} = V_1 \exp(-\sigma_1 n_0 z), \quad (4.4)$$

$$\left. \frac{dW_1}{d\tau} \right|_{\tau=0} = \frac{g+1}{g} V_1^2 \exp(-\sigma_1 n_0 z) [1 - \exp(-\sigma_1 n_0 z)]. \quad (4.5)$$

Equation (4.3) is convenient because the total number N_i of ions produced during the laser pulse in a cell of length l and unit cross section can be expressed in terms of the solution $W_1(\tau, l)$ (see Appendix):

$$\begin{aligned} N_i = \frac{V}{\sigma_1 B} \left[\sigma_1 n_0 l + \ln \frac{W_1}{V_1} + \frac{g+1}{(g+1)A+B} \frac{1}{W_1} \frac{dW_1}{d\tau} \right. \\ \left. - \frac{(g+1)^2}{g} \frac{V_1 - W_1}{(g+1)A+B} \right] \quad \text{for } z=l, \tau=\tau_p. \end{aligned} \quad (4.6)$$

We shall now consider two different cases.

1) Let us suppose that the optical thickness of the cell is so large that the medium does not transmit radiation corresponding to the second step during the laser pulse, i. e.,

$$W_1(\tau, l) \ll V_1, \quad A+B. \quad (4.7)$$

Equation (4.3) is then simplified and can be integrated. The approximate solution is

$$W_1 \approx V_1 \exp \left\{ -\sigma_1 n_0 l + \frac{B}{A+B} V_1 \tau + \left(\frac{g+1}{g} - \frac{B}{A+B} \right) \frac{V_1}{A+B} [1 - e^{-(A+B)\tau}] \right\}. \quad (4.8)$$

Because of the rapid exponential dependence in (4.8), the condition for this to be valid is

$$\sigma_1 n_0 l > \frac{V_1}{A+B} \left(B \tau_u + \frac{g+1}{g} \right) \quad \text{for } (A+B) \tau_p > 1, \quad (4.9)$$

$$\sigma_1 n_0 l > \frac{g+1}{g} V_1 \tau_u \quad \text{for } (A+B) \tau_p < 1. \quad (4.10)$$

The number of ions obtained in this case is given by

$$N_i \approx \frac{V_1 V_2}{\sigma_1 (A+B)} \left(\tau_p - \frac{1}{A+B} [1 - \exp\{-(A+B)\tau_p\}] \right). \quad (4.11)$$

As can be seen, it is independent of the density of atoms. This has a simple physical interpretation: all the photons corresponding to the first-step radiation are absorbed in the cell. In the limiting case of strong saturation at the second step ($V_2 \gg 1/\tau_p$, $A+A^*$), the number of ions is simply equal to the number of first-step photons.

2) Let us now consider the case where the medium transmits and this can be due to two factors, namely, photoionization of most of the atoms interacting with the radiation, and transmission through the working transition. Suppose that the medium begins to transmit at time τ_1 after the beginning of the pulse ($\tau_1 < \tau_p$). A possible case is

$$(A+B) \tau_1 \gg 1. \quad (4.12)$$

Since, under the actual experimental conditions $(A+A^*)\tau_p \ll 1$, the inequality given by (4.12) is equivalent to $V_2 \tau_1 \gg 1$, i. e., it is possible only for relatively high second-step laser power. The medium then transmits with the inequality (4.9) violated.

It is readily shown that the transmission time τ_1 is given by

$$\tau_1 \approx \sigma_1 n_0 l / V_1. \quad (4.13)$$

The number of ions produced at time τ_1 is

$$N_i \approx n_0 l, \quad (4.14)$$

i. e., practically all the atoms interacting with the radiation are ionized. The transmission of the medium is due to complete photoionization. The conditions under which this occurs can be obtained from (4.12) and (4.13):

$$V_2 \sigma_1 n_0 l / V_1 \gg 1, \quad \sigma_1 n_0 l / V_1 < \tau_p. \quad (4.15)$$

Let us now suppose that the transmission time τ_1 is such that the opposite condition is satisfied:

$$(A+B) \tau_1 \ll 1 \quad (\tau_1 < \tau_p). \quad (4.16)$$

It is clear that, in this case, the transmission of the medium can only occur through the working transition alone. One can then readily show from (4.10) that the transmission time is given by

$$\tau_1 \approx \frac{g}{g+1} \frac{\sigma_1 n_0 l}{V_1}. \quad (4.17)$$

The number of ions produced at this time can be found from (4.11):

$$N_i \approx n_0 l \left(\frac{g}{g+1} \right)^2 \frac{V_2 \sigma_1 n_0 l}{2V_1}. \quad (4.18)$$

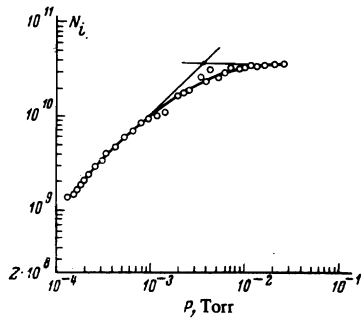


FIG. 4. Total number of recorded ions as a function of rubidium-atom density in the cell ($U=200$ V/cm; $\nu_1=23\,799$ cm^{-1} , $\nu_2=14\,403$ cm^{-1}).

The conditions for transmission through the working transition can be found from (4.16) and (4.17)

$$\frac{g}{g+1} \frac{(A+B)\sigma_1 n_0 l}{V_1} \ll 1, \quad \frac{g}{g+1} \frac{\sigma_1 n_0 l}{V_1} < \tau_p. \quad (4.19)$$

It is clear that we then have

$$N_i(\tau_i)/n_0 l \ll 1. \quad (4.20)$$

i. e., the relative fraction of atoms that are ionized at the transmission time τ_1 is small. From the time τ_1 onward, the medium transmits, i. e., $n_1 \approx n_2/g$.

The first two equations in (4.1) readily yield the following formula for the total number of ions during the laser pulse:

$$N_i = n_0 l \frac{V_2}{B} \left[1 - e^{-\gamma} + \left(\frac{g}{g+1} \right)^2 \frac{B\sigma_1 n_0 l}{2V_1} e^{-\gamma} \right], \quad (4.21)$$

where

$$\gamma = \frac{g}{g+1} B \left(\tau_p - \frac{g}{g+1} \frac{\sigma_1 n_0 l}{V_1} \right). \quad (4.22)$$

5. ION YIELD

Dependence on the density of atoms

The experimental dependence of the total recorded number of ions on the density of rubidium atoms in the cell is shown in Fig. 4. This dependence is linear for densities in the range $2 \times 10^{12} - 2 \times 10^{13}$ cm^{-3} , and eventually becomes saturated as the rubidium vapor density increases. In accordance with the theory, therefore,

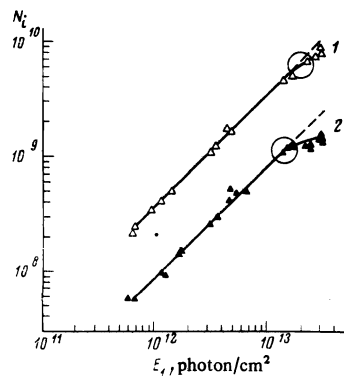


FIG. 5. Total number of recorded ions as a function of the exciting-radiation intensity: curve 1—rubidium-vapor density in the cell $N_0 = 4.5 \times 10^{13}$ cm^{-3} ; curve 2— $N_0 = 1.4 \times 10^{13}$ cm^{-3} .

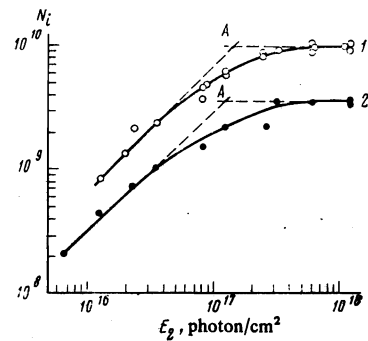


FIG. 6. Total number of recorded ions as a function of ionizing radiation intensity I_2 with ruby laser radiation used for ionization: curve 1— $U=2.4$ kV/cm; curve 2— $U=1$ kV/cm ($\nu_1 = 23\,799$ cm^{-1} , $\nu_2 = 14\,403$ cm^{-1} , $N_0 = 3.2 \times 10^{13}$ cm^{-3}).

two cases are realized in this range of densities: (1) all the laser radiation corresponding to the first step is absorbed within the detection length l , and the total number of ions is determined by the number of first-step photons, but is independent of the density of the rubidium atoms [formula (4.11) subject to (4.9) and (4.10)]—this is the plateau on the curve; (2) the medium transmits, and the total number of ions is determined by the rubidium-vapor density in the cell [formula (4.12) subject to (4.15) and (4.19)]—this is the linear part of the curve. The point at which the curve reaches the plateau in Fig. 4 is determined by $\sigma_1 n_0^l \sim V_1 \tau_p$.

It is important to note, however, that the quantity n_0 differs from the rubidium-atom density N_0 in the cell. This is due to the presence of fine structure (mode structure and the structure due to additional selection) in the first-step laser line, so that only a fraction of the atoms within the Doppler profile can interact with the laser radiation, i. e., $n_0 = N_0 \Delta\nu_M / \nu_D$, where $\Delta\nu_D$ is the Doppler width of the rubidium absorption line, $\Delta\nu_M = \alpha \Delta\nu_M^0$, α is the number of modes within the Doppler profile, and $\Delta\nu_M^0$ is the width of a single mode. These parameters have the following numerical values:

$$\Delta\nu_D = 3.6 \cdot 10^{-2} \text{ cm}^{-1}, \quad E_1 = V_1 \tau_p / \sigma_1 = 2.9 \cdot 10^{13} \text{ photon/cm}^2, \\ \sigma_1 = 3.2 \cdot 10^{-13} \text{ cm}^2 [^{16}], \quad l = 2.5 \text{ cm}.$$

From the condition for the onset of saturation (Fig. 4), we have $n_0 = 1.2 \times 10^{13}$ cm^{-3} and hence the optical thickness of the rubidium-vapor layer at this point is $L = \sigma_1 n_0 l = 9.3$. The experimental curve in Fig. 4 yields $N_0 = 7 \times 10^{13}$ cm^{-3} , i. e., $\Delta\nu_M / \Delta\nu_D = 0.17$.

Dependence on radiation intensities

Figures 5–7 show the typical ion yield as a function of the intensity of the exciting ($\nu_1 = 23\,799$ cm^{-1}) and ionizing ($\nu_2 = 14\,403$ and $28\,806$ cm^{-1}) radiations. Results of this type were obtained in a broad range of rubidium-atom density in the cell and for different extracting fields. It was found that, in the range of density and exciting and ionizing intensity that we have investigated, a change in the extracting field resulted in a change in only the absolute yield of ions, but the shape of the curves remained unaltered.

The dependence of the ion yield on the intensity of the exciting radiation is shown in Fig. 5 for different ru-

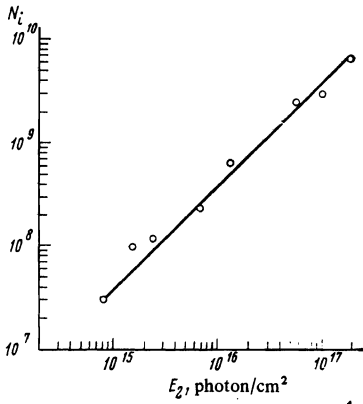


FIG. 7. Total number of ions as a function of the intensity of ionizing radiation using the second harmonic of the ruby laser ($\nu_1 = 23\,799\text{ cm}^{-1}$, $\nu_2 = 28\,806\text{ cm}^{-1}$, $N_0 = 3 \times 10^{13}\text{ cm}^{-3}$).

rubidium-atom densities in the cell. For low radiation intensities, the ion yield is a linear function of the first-step laser radiation intensity, but a departure from linearity is observed at higher intensities. An increase in the rubidium-vapor density returns this to a linear dependence.

This behavior of the curves in Fig. 5 is explained satisfactorily by the theoretical model considered above. Thus, when the attenuation of the intensity of exciting radiation corresponding to the first step is insufficient to produce transmission in the medium, i. e., when conditions (4.15) and (4.19) are violated, all the exciting photons are absorbed within the length of the recording system and, consequently, the yield of ions is determined by the number of absorbed photons [formula (4.11)]. When the rubidium-atom density is high, on the other hand, so that conditions (4.9) and (4.10) are satisfied throughout the range of radiation intensity, the dependence becomes linear for all these intensities. The points at which departure from linearity should occur can readily be obtained from the condition $\sigma_1 n_0 l \sim V_1 \tau_p$ [see (4.9) and (4.10)]. The position of these points is indicated by the large circles in Fig. 5.

The yield of ions as a function of the intensity of the ionizing radiation is shown in Figs. 6 and 7 ($\nu_2 = 14\,403$ and $28\,806\text{ cm}^{-1}$, respectively). At low intensities of the ionizing radiation, the dependence is linear (Fig. 6) but, as the intensity increases, the straight line turns over and reaches saturation in which each selectively excited atom is transformed into an ion.

In the case of ionization by radiation of frequency $\nu_2 = 28\,806\text{ cm}^{-1}$, there is no saturation (Fig. 7) and the dependence remains linear for all intensities I_2 .

Let us now determine the point at which saturation is reached in Fig. 6. We shall do this as follows: we continue the linear part of the curve until it cuts the plateau by extension (shown by the broken line in Fig. 6). Analysis of the experimental yield of ions as a function of the second-step intensity I_2 ($\nu_2 = 14\,403\text{ cm}^{-1}$) shows that the position of the point A defined in this way does not depend on the intensity of the exciting radiation I_1 ($\nu_1 = 23\,799$ and $23\,725\text{ cm}^{-1}$) in each of the intervals

$$(\sigma_1 n_0 l < V_1 \tau_p \text{ and } \sigma_1 n_0 l > \tau_p).$$

Let us now consider the case where complete absorption of the exciting radiation I_1 occurs within the length l of the recording system [see (4.9) and (4.10)]. The ion yield is then given by (4.11), which takes the following form in the two limiting cases:

$$N_i/E_1 \approx \sigma_2 E_2/2, \quad \sigma_2 E_2 \ll 1; \quad (5.1)$$

$$N_i/E_1 \approx 1, \quad \sigma_2 E_2 \gg 1 \quad (5.2)$$

($A\tau_p \approx 0.17$). Thus, at low intensities of ionizing radiation, $\sigma_2 E_2 \ll 1$, the ion yield is linear as a function of I_2 and reaches the plateau for $\sigma_2 E_2 \gg 1$, which is determined by the total number E_1 of exciting photons. The point A in Fig. 6, defined as the point of intersection of (5.1) and (5.2), is then given by

$$\sigma_2 E_2 \approx 2. \quad (5.3)$$

A similar analysis of the ion yield N_i as a function of ionizing intensity I_2 in the case when the medium transmits [Eqs. (4.14), (4.21), (4.22) subject to (4.15) and (4.19)] yields the following condition for the point A:

$$\sigma_2 E_2 \approx (g+1)/g \quad (5.4)$$

($g = 2$ and 1 for the $6^2P_{3/2}$ and $6^2P_{1/2}$ levels, respectively).

Thus, in complete agreement with the experimental results, the point A on the curve showing the ion yield as a function of the ionizing radiation intensity is independent of the intensity of the exciting radiation and is given by (5.3) and (5.4).

6. CROSS SECTIONS FOR THE PHOTOIONIZATION OF THE RUBIDIUM ATOM FROM THE EXCITED STATE 6^2P

The experimental and theoretical analysis of the yield of ions as a function of the intensity of ionizing radiation has shown that the point at which the plateau is reached (point A in Fig. 6) is independent of the intensity of the exciting radiation and is given by (5.3) and (5.4). This provides us with a simple method of determining the cross sections for the photoionization of atoms from excited states. The photoionization cross section is determined only by the total number E_2 of photons in the ionizing beam at the point A at which the curve reaches saturation (Fig. 6), and does not require any information about the absolute number of excited atoms.

We have used this method to determine the cross sections for the photoionization in the $6^2P_{3/2}$ and $6^2P_{1/2}$ states by ruby laser radiation. The average cross section obtained for ten measurements on the $6^2P_{3/2}$ level was found to be $(1.7 \pm 0.3) \times 10^{-17}\text{ cm}^2$. The absolute uncertainty is largely determined by uncertainties in the measured radiation energy and was estimated to be $0.3 \times 10^{-17}\text{ cm}^2$. The corresponding result for the $6^2P_{1/2}$ state is $(1.5 \pm 0.3) \times 10^{-17}\text{ cm}^2$ (see table).

In the case of ionization by second-harmonic radiation, the cross sections were determined by comparing the slope of the corresponding graph (Fig. 7) with the slope of the linear part of the curve obtained by ionization with the fundamental-frequency ruby radiation (Fig. 6) under identical experimental conditions. The

State of atom*	ν_1, cm^{-1}	$\sigma_2 \cdot 10^{17}, \text{cm}^2$	
		Experiment	Calculation
$6^2P_{3/2}(23799)$	14 403	1.7 ± 0.3	0.95
$6^2P_{1/2}(23725)$	14 403	1.5 ± 0.3	0.95
$6^2P_{3/2}(23799)$	28 806	0.19 ± 0.03	0.3

*The figure in parentheses indicates the value of the excitation frequency ν_1, cm^{-1} .

cross section for photoionization from the $6^2P_{3/2}$ state in the case of ionization with $\nu_2 = 28 806 \text{ cm}^{-1}$ is $(1.09 \pm 0.3) \times 10^{-18} \text{ cm}^2$. Calculations of the photoionization cross section for the 6^2P state of the rubidium atom based on Burgess-Seaton formula^[16] were found to be in good agreement with the measured values (see table).

7. CONCLUSIONS

Two characteristics are the most important for the process of selective two-step photoionization of atoms by laser radiation: the degree to which the ionization and the extraction of a given species from the mixture is selective, and the probability of ionization of atoms belonging to the selected species during the interaction with the light field. In this paper, we have investigated the second characteristic. We have analyzed the relevant conditions and have demonstrated the possibility that each of the selected atoms will be ionized during a single radiation pulse and sufficiently high ion density will be produced ($\sim 10^{12} \text{ cm}^{-3}$). The method of two-step photoionization under saturation conditions has also been found to be effective as a means of measuring the cross sections for photoionization from excited states. Our work has shown the importance of choosing the transition scheme for ionization with maximum cross section. Phototransitions into the continuum have the common defect that the photoionization cross section is low even under optimal conditions. There is, therefore, considerable interest, in our view, in investigating ionization schemes using coupled autoionization states, especially autoionization of highly excited states of atoms in electric fields.^[17] Recent experiments^[18] have demonstrated the efficacy of this approach.

APPENDIX

Let us transform (4.1) to a more convenient form. To do this, let us differentiate the third equation with respect to $\tau = t - z/c$. Simple rearrangement then yields, in the notation of (4.2),

$$\frac{\partial}{\partial z} \left(\frac{1}{W_1} \frac{\partial W_1}{\partial \tau} \right) = -\frac{g+1}{g} \frac{\partial W_1}{\partial z} - \sigma_1 \left[\frac{(g+1)A+B}{g} \right] n_2. \quad (\text{A.1})$$

Differentiating again with respect to τ and using the second and third equations in (4.1) together with (A.1), we obtain the following equation for W_1 which contains the complete differential with respect to z :

$$\frac{\partial^2}{\partial z \partial \tau} \left(\frac{1}{W_1} \frac{\partial W_1}{\partial \tau} \right) + \frac{g+1}{g} \frac{\partial^2 W_1}{\partial z \partial \tau} + (A+B) \frac{\partial}{\partial z} \left(\frac{1}{W_1} \frac{\partial W_1}{\partial \tau} \right) + B \frac{\partial W_1}{\partial z} = 0. \quad (\text{A.2})$$

It is clear that this equation can be integrated with respect to z . The integration constant will, in general, be a function τ . It can be found from the additional condition that the pulse has a given form on the boundary

$z=0$. In our case, the integration constant is equal to BV_1 on the time interval $(0 < \tau < \tau_p)$ and this yields (4.3).

The second-order equation given by (4.3) should have two initial conditions. The first initial condition (4.4) is found by direct integration of the third equation in (4.1) with respect to z . The second initial condition for the value of the derivative for $\tau=0$ can be found by integrating (A.1) with respect to z . Using the specified shape of the pulse on $z=0$, this yields:

$$\frac{1}{W_1} \frac{dW_1}{d\tau} = \frac{g+1}{g} (V_1 - W_1) - \sigma_1 \left[\frac{(g+1)A+B}{g} \right] \int_0^l n_2 dz', \quad (\text{A.3})$$

and hence we obtain (4.5).

Let us now express the total number $N_i(\tau)$ of ions in a cell of length l and unit transverse cross section in terms of the function $W_1(\tau, l)$. It is clear that

$$N_i(\tau) = \frac{V_2}{B} \left[n_0 l - \int_0^l (n_1 + n_2) dz \right]. \quad (\text{A.4})$$

The third equation in (4.1) yields

$$\int_0^l n_1 dz - \frac{1}{g} \int_0^l n_2 dz = -\frac{1}{\sigma_1} \ln \frac{W_1}{V_1} \Big|_{z=0}^l. \quad (\text{A.5})$$

Combining this with (A.3), we finally obtain the expression for $N_i(\tau)$ given by (4.6).

- ¹R. V. Ambartsumyan and V. S. Letokhov, IEEE J. Quantum Electron. QE-7, 305 (1971); Appl. Opt. 11, 354 (1972).
- ²R. V. Ambartsumyan, V. P. Kalinin, and V. S. Letokhov, Pis'ma Zh. Eksp. Teor. Fiz. 13, 305 (1971) [JETP Lett. 13, 217 (1971)].
- ³V. S. Letokhov, Opt. Commun. 7, 59 (1973).
- ⁴B. B. Snavely, Inv. Review of the Eighth Intern. Conf. on Quantum Electronics, San Francisco, 1974.
- ⁵U. Brinkmann, W. Hartig, H. Telle and H. Walther, Appl. Phys. 5, 109 (1974).
- ⁶D. J. Bradley, P. Ewart, J. V. Nicholas, J. R. D. Shaw, and D. G. Thompson, Phys. Rev. Lett. 31, 263 (1973).
- ⁷Experiments With Molecular Beams, Collection of Translations ed. by A. M. Brodskii (Russ. Transl., Mir, M., 1969).
- ⁸C. H. Corliss and W. R. Bozman, Transition Probabilities and Oscillator Strengths of 70 elements (Russ. Trans.) Mir, M., 1968.
- ⁹G. V. Marr, Photoionization Processes in Gases, Academic Press, New York-London, 1967.
- ¹⁰K. J. Nygaard and R. E. Hebner Jr, Paper read at the Seventh Intern. Conf. on the Physics of Electr. and Atom. Coll., Amsterdam, 1971.
- ¹¹A. I. Klyucharev and I. S. Ryazanov, Opt. Spektrosk. 32, 1253 (1972) [Opt. Spectrosc. (USSR) 32, 686 (1972)]; A. I. Klyucharev and V. Yu. Sepman, Opt. Spektrosk. 38, 1230 (1975).
- ¹²T. W. Hänsch, Appl. Opt. 11, 895 (1972).
- ¹³O. V. Kozlov, Elektronnyi zond v plazme (Electron Probe in Plasma), Atomizdat, 1969.
- ¹⁴Sb. Voprosy teorii plazmy (in: Problems in the Theory of Plasma) ed. by M. A. Leontovich, No. 1, Gosatomizdat, 1963.
- ¹⁵V. S. Letokhov and A. A. Makarov, J. Photochemistry 2, 421 (1974).
- ¹⁶A. Burgess and M. J. Seaton, Monthly Not. Roy. Astron. Soc. 120, 121 (1960).
- ¹⁷L. N. Ivanov and V. S. Letokhov, Kvantovaya Elektron. (Moscow) 2, 585 (1975) [Sov. J. Quantum Electron. 5, 329 (1975)].
- ¹⁸R. V. Ambartsumyan, G. I. Bekov, V. S. Letokhov, and V. I. Mishin, Pis'ma Zh. Eksp. Teor. Fiz. 21, 595 (1975) [JETP Lett. 21, 279 (1975)].

Translated by S. Chomet